Pflugers Arch - Eur J Physiol (2013) 465:839–851
DOI 10.1007/s00424-012-1196-6

Substitution of transmembrane domain Cys residues alters pH_o-sensitive anion transport by AE2/SLC4A2 anion exchanger

Fabian R. Reimold · Andrew K. Stewart · Kathleen Stolpe · John F. Heneghan · Boris E. Shmukler · Seth L. Alper

Received: 6 September 2012 / Revised: 19 November 2012 / Accepted: 30 November 2012 / Published online: 28 December 2012

Abstract AE2/SLC4A2 is the most widely expressed of the Na^+-independent SLC4 Cl^-/HCO_3^- exchangers and is essential for postnatal survival, but its structure remains unknown. We have generated and expressed a mouse AE2 construct devoid of transmembrane domain cysteine (Cys) residues, $mAE2_{Cys\text{-}less}$, to enhance the utility of Cys-substitution mutagenesis for structural and structure–function studies of mAE2. $mAE2_{Cys\text{-}less}$ expressed in *Xenopus* oocytes exhibited partial reduction of stilbene disulfonate-sensitive anion exchange activity. This activity was independent of the mAE2 N-terminal cytosolic domain and was accompanied by near-normal surface expression, without change in $K_{1/2}$ for extracellular Cl^-. $mAE2_{Cys\text{-}less}$ exhibited wildtype activation of anion exchange by hypertonicity and by NH_4Cl, and wildtype inhibition of anion exchange by acidic intracellular pH (pH_i) in the absence of NH_4^+. However, inhibition of anion exchange by extracellular pH (pH_o) exhibited an alkaline shifted $pH_{o(50)}$ value of at least 0.6–0.7 pH units. Although SO_4^{2-} transport by $mAE2_{Cys\text{-}less}$ resembled wildtype mAE2 in its stimulation by acidic pH_o, the absence of transmembrane domain Cys residues abrogated activation of oxalate transport by acidic pH_o. The contrasting enhancement of SO_4^{2-} transport by alkaline pH_o in the mAE1 anion translocation pathway mutant E699Q (*Am J Physiol Cell Physiol* 295: C302) was phenocopied by the corresponding mutant E1007Q in both AE2 and $AE2_{Cys\text{-}less}$. However, the absence of transmembrane domain Cys residues exacerbated the reduced basal anion transport function exhibited by this and other missense substitutions at AE2 residue E1007. $AE2_{Cys\text{-}less}$ will be a valuable experimental tool for structure–function studies of the SLC4 gene family, but its utility for studies of AE2 regulation by extracellular pH must be evaluated in the context of its alkaline-shifted pH_o sensitivity, resembling that of AE2 gastric parietal cell variant AE2c1.

Keywords *Xenopus* oocyte · Chloride–bicarbonate exchanger · Oxalate · pH dependence · Hypertonicity · Ammonium

Introduction

The SLC4 gene superfamily encodes three Na^+-independent, Cl^-/HCO_3^- exchangers (SLC4A1-3), five Na^+-dependent HCO_3^- cotransporters or exchangers (SLC4A4, A5, A7, A8, and A10), a borate efflux transporter (SLC4A11), and SLC4A9, of still uncertain function. Mutations in human SLC4A1 cause hereditary spherocytic and stomatocytic anemias and familial distal renal tubular acidosis. A coding polymorphism in SLC4A3 is associated with susceptibility to seizure disorder. Mutations in SLC4A4 cause proximal renal tubular acidosis. Mutations in human SLC4A11 cause late-onset blindness due to several clinical variants of corneal endothelial dystrophy. Mouse knockouts of other SLC4 transporters produce additional disease phenotypes in mice [2, 3].

Although deficiency of AE2 has not yet been associated with Mendelian human disease, the $Ae2^{-/-}$ mouse dies within 3–4 weeks after birth, and suffers osteopetrosis [51], hypochlorhydria, and intestinal hyposecretion [15, 16]. The hypomorphic $Ae2^{a,b-/-}$ mouse is grossly normal but exhibits male infertility [32], less severe bone disease [24],

Electronic supplementary material The online version of this article (doi:10.1007/s00424-012-1196-6) contains supplementary material, which is available to authorized users.

F. R. Reimold · A. K. Stewart · K. Stolpe · J. F. Heneghan · B. E. Shmukler · S. L. Alper (✉)
Renal Division and Molecular and Vascular Medicine Division, Beth Israel Deaconess Medical Center, 99 Brookline Avenue, RN-380F,
Boston, MA 02215, USA
e-mail: salper@bidmc.harvard.edu

and serological signs reminiscent of human primary biliary cirrhosis [38].

SLC4A2/AE2 differs in its regulation from the more extensively studied SLC4 polypeptide SLC4A1/AE1 in several important ways. AE2-mediated Cl^- transport is inhibited by intracellular and, independently, by extracellular protons in the physiological range, whereas Cl^- transport by AE1 is inhibited only at non-physiologically acidic pH values [44, 56]. AE2 is activated by hypertonicity, but AE1 is insensitive to the same range of tonicity [23]. AE2 is activated by NH_4^+, despite its intracellular acidification of *Xenopus* oocytes, but AE1 is NH_4^+-insensitive [21]. The transmembrane domain of AE2 contributes importantly to these regulatory processes [10], but the relationship of residues controlling these regulatory processes to the still incompletely defined bidirectional anion translocation pathway remains unclear.

Structural information for the SLC4 gene family will thus be of substantial functional importance in understanding the varied transport mechanisms and substrate specificities exhibited by these widely expressed, phylogenetically ancient, SLC4 polypeptides. The crystal structure of part of the erythroid SLC4A1/AE1 N-terminal cytoplasmic domain has been reported [54], but the available structural information for the AE1 transmembrane domain is of inadequate resolution (7.5 A) for visualization of all transmembrane helices [52]. Cysteine scanning mutagenesis has provided important information on topographical accessibility and structure–function relationships for SLC4A1 [50, 59, 60, 63] and SLC4A4 [31, 58, 61, 62]. Interpretation of the mutagenesis data has been simplified for human SLC4A1 by the availability of variants in which all Cys residues (or, in the case of trout AE1, all transmembrane domain Cys residues) have been mutated to Ser [6, 30]. A preliminary report of Cys-less SLC4A4 has also appeared [64]. However, systematic Cys substitution and scanning mutagenesis studies of AE2 have not been reported. The substantial differences in regulation between AE1 and AE2 suggest structural differences expected to inform investigations of structure–function relationships across the ten-member SLC4 gene family.

We therefore generated a mouse AE2 (mAE2) expression construct in which all transmembrane domain cysteines have been substituted either with residues found in corresponding positions of AE1 and/or AE3, or with Ser or Ala.

Expression of this Cys-less mAE2 ($mAE2_{Cys\text{-}less}$) in *Xenopus* oocytes revealed preservation of DIDS-sensitive anion exchange at the oocyte cell surface, with apparent AE2 affinity for extracellular Cl^- indistinguishable from that of wildtype AE2. $mAE2_{Cys\text{-}less}$ also preserved wildtype activation by hypertonicity and by NH_4^+, and maintained wildtype inhibition by acidic intracellular pH (pH_i). However, the absence of transmembrane Cys residues enhanced the sensitivity of Cl^- transport to inhibition by extracellular protons, such that the pH_o at which inhibition was 50 % of maximum ($pH_{o(50)}$) was >0.6–0.7 pH units higher than that of wildtype AE2. Missense substitution of all transmembrane domain Cys residues preserved both activation by extracellular protons of mAE2-mediated SO_4^{2-} transport and the contrasting activation by alkaline pH_o of mAE2 E1007Q-mediated SO_4^{2-} transport. However, absence of transmembrane domain Cys residues abolished pH sensitivity of mAE2-mediated oxalate transport. The lack of transmembrane domain Cys residues also potentiated the reduction of Cl^- transport by the mAE2 anion translocation pathway mutant E1007Q and by polypeptides carrying other substitutions at the same position.

Methods

Materials

$Na^{36}Cl$ and $Na_2{}^{35}SO_4$ were from Perkin-Elmer (Waltham, CA). ^{14}C oxalate was from NEN-DuPont (gift of C. Scheid and T. Honeyman, University of Massachusetts Medical Center). Restriction enzymes were from New England Biolabs (Beverly, MA). EXPAND high-fidelity PCR System and T4 DNA ligase were from Roche Diagnostics (Indianapolis, IN). 4,4′-Diisothiocyanostilbene-2,2′-disulfonic acid (DIDS) was obtained from Calbiochem (La Jolla, CA). Other chemicals (of reagent grade) were from Sigma (St. Louis, MO) or Fluka (Milwaukee, WI).

Solutions

MBS consisted of (in mM) 88 NaCl, 1 KCl, 2.4 $NaHCO_3$, 0.82 $MgSO_4$, 0.33 $Ca(NO_3)_2$, 0.41 $CaCl_2$, and 10 HEPES (pH 7.40). ND-96 consisted of (in mM) 96 NaCl, 2 KCl, 1.8 $CaCl_2$, 1 $MgCl_2$, and 5 HEPES (pH 7.40). In ND-96 at pH 5 and 6, Na HEPES was replaced by equimolar MES. In Cl^--free or partially Cl^--substituted solutions, NaCl was replaced mole for mole with Na cyclamate. Cl^- salts of K^+, Ca^{2+}, and Mg^{2+} were substituted on an equimolar basis with the corresponding gluconate salts as needed. In some experiments 30 mM NaCl was replaced with 20 mM Na_2SO_4 as indicated. Oxalate-containing bath solutions were nominally Ca^{2+}-free. Addition to flux media of the weak acid sodium butyrate (40 mM) was in equimolar substitution for Na cyclamate. Bath addition of NH_4Cl (26 mM) was in equimolar substitution for NaCl.

cDNA mutagenesis

Mouse SLC4A2a/AE2a (mAE2) cDNA was subcloned into the *Xenopus* oocyte expression vector pXT7. All transmembrane

domain Cys residues were subjected to missense mutagenesis by four primer polymerase chain reaction (PCR) as described [18, 47] to generate $AE2_{Cys\text{-}less}$. AE2 C704 was changed to Val, C751 and C1042 were changed to Ala (as in the corresponding residues of mAE1), and C1211 was changed to Ala (as in AE3). AE2 C778 (highly conserved) and C851 (in the AE2-specific sequence of the third extracellular loop) were changed to Ser. Highly conserved AE2 C1169 and unconserved C1224 were also changed to Ala. $AE2_{Cys\text{-}less(7/8)}$ lacked all transmembrane domain Cys residues except C1211. Oligonucleotide primer sequences are presented in Table S1. PCR-amplified products were sequenced in entirety to ensure absence of unintended mutations. The sites of missense mutations in $AE2_{Cys\text{-}less}$ are summarized in Fig. 1. We define the "transmembrane domain" as extending from the start of TM1 to the C terminus and including, in addition to lipid bilayer-spanning or -embedded regions, all extracellular and intracellular loops and the cytoplasmic C-terminal tail.

cRNA expression in Xenopus oocytes

Capped cRNA was transcribed from linearized cDNA templates with Megascript T7 RNA polymerase kit (Ambion, Austin, TX) and purified with an RNeasy mini-kit (Qiagen, Germantown, MD). cRNA concentration (A_{260}) was measured by Nanodrop spectrometer (ThermoFisher, Waltham, MA), and integrity was confirmed by formaldehyde agarose gel electrophoresis. Mature female *Xenopus laevis* frogs (Department of Systems Biology, Harvard Medical School) were subjected to partial ovariectomy under hypothermic tricaine anesthesia following protocols approved by the Institutional Animal Care and Use Committee (IACUC) of Beth Israel Deaconess Medical Center. Stage V–VI oocytes were prepared by overnight incubation of ovarian fragments in MBS with 1.5 mg/ml collagenase B (Alfa Aesar, Ward Hills, MA), followed by a 20 min rinse in Ca^{2+}-free MBS, with subsequent manual selection and defolliculation as needed. Oocytes were injected on the same day with cRNA (0.5–50 ng as indicated), and maintained 72 h at 17.5 °C in MBS containing 10 μg/ml gentamicin until used for experiments. As uninjected and water-injected oocytes did not differ in anion transport at 72 h post-injection (data not shown), uninjected oocytes were used as controls for the current experiments.

Isotopic influx experiments

Unidirectional $^{36}Cl^-$ influx studies were carried out for periods of 30 min in 148 μl ND-96 and 2 μl of carrier-free 260 mM $Na^{36}Cl^-$ (0.25 μCi), resulting in total bath $[Cl^-]$ of 103.6 mM. In experiments testing the effect of NH_4^+ on $^{36}Cl^-$ influx, ND-96 was substituted with ND-70 plus 26 mM NH_4Cl. In experiments testing the effect of hypertonicity on $^{36}Cl^-$ influx, ND-96 (212 mOsm) was supplemented with mannitol to achieve calculated osmolarities of 280 or 400 mOsm, maintaining constant $[Cl^-]$. In all $^{36}Cl^-$

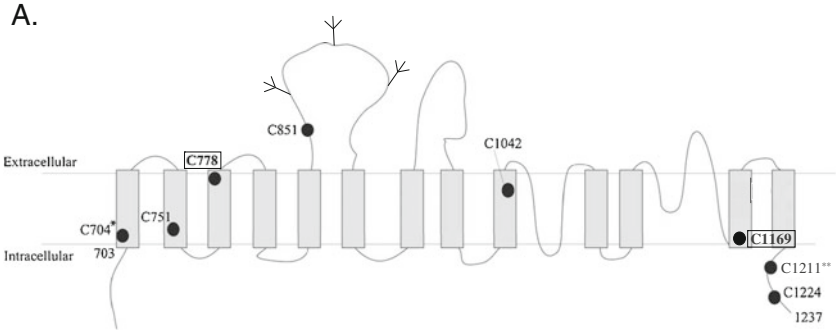

B.

SLC4 anion exchanger								
$mAE2_{Cys\text{-}less}$	C704V	C751A	**C778S**	C851S	C1042A	**C1169A**	**C1211A**	C1224A
mAE2 wt	C704	C751	**C778**	C851	C1042	**C1169**	**C1211**	C1224
hAE1 wt	V405	A452	**C479**	T552	A716	**C843**	**C885**	E898
$hAE1_{Cys\text{-}less}$			**C479S**			**C843S**	**C885S**	

Fig. 1 Cysteine residues of the transmembrane domain of mouse AE2. **a** Schematic of mAE2 Cys residues. *Numbered black circles* indicate Cys residues. *Boxed bold* indicates Cys conservation among all SLC4 polypeptides (C778, C1169). C704 (*) is conserved in mAE3 but not mAE1. C1211 (**) is conserved in mAE1, but not mAE3. Other Cys residues are conserved among only mammalian AE2 polypeptides or (for 1224 only) not conserved. Consensus *N*-glycosylation sites are indicated in the third extracellular loop. **b** Comparison of mAE2 transmembrane domain Cys residues with the corresponding residues of hAE1. The mutagenic oligonucleotides and their encoded missense substitutions are presented in Table S1. The topographic model is derived from Zhu et al. (62)

influx experiments the carrier solution was supplemented with 10 μM bumetanide to impair Cl^- influx by native oocyte NKCC1.

Unidirectional $^{35}SO_4^{2-}$ influx studies were carried out for periods of 30 min in a bath containing 148 μl of a carrier solution consisting of (in mM) 20 Na_2SO_4, 76 Na cyclamate, 2 K glutamate, 1.8 Ca glutamate, 1 Mg glutamate, and 2 μl of carrier-free $^{35}SO_4^{2-}$ (2 μCi, 47 nM) [18]. pH 5.0 solutions were buffered with 5 mM MES, and pH 8.0 solutions were buffered with 5 mM HEPES. Unidirectional ^{14}C oxalate influx studies were carried out for 30 min periods in 148 μl of nominally Ca^{2+}- and Mg^{2+}-free influx medium containing (in mM) 96 mM Na cyclamate, 2 K glutamate, with 2 μl carrier-free 100 mM ^{14}C oxalate (0.75 μCi), resulting in a final ^{14}C oxalate concentration of 1.3 mM. pH 5.0 solutions were buffered with 5 mM MES, and pH 8.0 solutions were buffered with 5 mM HEPES.

Influx experiments were terminated with four washes in ice-cold isotonic Na cyclamate solution (nominally Mg^{2+}- and Ca^{2+}-free for oxalate influx studies). Washed oocytes were individually lysed in 150 μl 2 % sodium dodecyl sulfate (SDS). Triplicate 10-μl aliquots of the influx solution were used to calculate specific acitivity of radiolabeled substrate anions. Oocyte anion uptake was calculated from cpm values of washed oocytes and from bath specific activity.

Isotopic efflux experiments

For unidirectional $^{36}Cl^-$ efflux studies, individual oocytes were injected with 50 nl of 260 mM $Na^{36}Cl$ (6.25 nCi, 20,000–24,000 cpm). Following a 5- to 10-min recovery period in Cl^--free solution (cyclamate), the efflux assay was initiated by transfer of individual oocytes to 6-ml borosilicate glass tubes, each containing 1 ml efflux solution. At intervals of 1 or 3 min, 0.95 ml of this efflux solution was removed for scintillation counting and replaced with an equal volume of fresh efflux solution. Following completion of the assay with a final efflux period either in Cl^--free cyclamate solution or in the presence of the inhibitor DIDS (200 μM unless otherwise noted), each oocyte was lysed in 150 μl of 2 % SDS. Samples were counted for 3–5 min such that the magnitude of 2SD was <5 % of the sample mean.

To vary pH_i at constant pH_o, oocytes were pre-exposed to 40 mM Na butyrate (substituting for Na cyclamate) for 30 min prior to initiation of an efflux experiment, producing intracellular acidification of 0.5 pH units [44]. Upon removal of bath butyrate (with substitution by Na cyclamate) during the course of the efflux experiment, pH_i rapidly alkalinized back towards initial pH_i ($t_{1/2}$=6 min), while pH_o remained constant. 40 mM butyrate is neither an inhibitor nor a substrate of AE2 [43].

Efflux data was plotted as the natural logarithm (ln) of the quantity (%cpm remaining in the oocyte) vs. time. Efflux rate constants for $^{36}Cl^-$ were measured from linear fits to data from the last three time points sampled within each experimental period. For each experiment, uninjected oocytes from the same frog were subjected to parallel measurements with cRNA-injected oocytes. Oocytes, with <15 % of injected $^{36}Cl^-$ remaining at the end of the assay were excluded from analysis [35]. Extracellular $[Cl^-]$ ($[Cl^-]_o$)–response curves were fit by the following Michaelis–Menten-type equation with baseline offset (Sigmaplot 11.0):

$$K_{\text{eff}} = \frac{y_0 + V_{\max} \times [\text{anion}]}{(K_{1/2} + [\text{anion}])} \quad (1)$$

where k_{eff} is the $^{36}Cl^-$ efflux rate constant, y_0 is the efflux rate constant in the absence of extracellular substrate anion (in the presence of nominally impermeant anions cyclamate and gluconate), $V_{\max}$ represents the maximal value of k_{eff}, and $K_{1/2}$ the $[Cl^-]_o$ at which k_{eff} is half-maximal.

The pH_o sensitivity of AE2-mediated $^{36}Cl^-$ efflux at nearly constant pH_i was measured and reproduced our previously reported data [44]. Individual oocytes were exposed sequentially to ND-96 at pH_o 5.0, 6.0, 7.0, 8.0, and 8.5, followed by addition of DIDS (200 μM) at pH_o 8.5. Rate constants measured at each pH_o value for each oocyte were fit with the following first order logistic sigmoid equation,

$$V = \left(V_{\max} \times 10^{-K}\right) / \left(10^{-K} + 10^{-X}\right) + d \quad (2)$$

where V, $V_{\max}$ are as defined above, exponent X is the pH_o at which the efflux rate constant was measured, exponent K is $pH_{o(50)}$ (pH_o at which V is half-maximal), and d is the efflux rate constant in the absence of substrate anion, with a value ≥0. Equation 2 allowed calculation (Microsoft Excel) of $V_{\max}$ and $pH_{o(50)}$ values for each individual oocyte. Rate constants measured at each pH_o value were normalized to that oocyte's $V_{\max}$ (set at 100 %). Mean normalized data for mAE2 and for $mAE2_{\text{Cys-less}}$ were fit (Sigma Plot version 11.0) to Eq. 2.

All experimental conditions were tested in oocytes from at least two frogs.

Confocal immunofluorescence microscopy

Oocytes were injected with cRNA encoding wildtype (10 ng) or mutant (50 ng) mAE2 bearing the HA epitope (YPYDVPDYA) inserted between Glu-858 and Ala-859 in the third extracellular loop. Uninjected oocytes and oocytes injected with cRNA 3 days prior were fixed at 4 °C for 30 min in phosphate-buffered saline (PBS) containing 1.5 % paraformaldehyde (PFA), then washed three times in PBS supplemented with 0.002 % sodium azide, exposed to 1 % SDS in 1× PBS for 5 min, and then blocked in PBS with 1 % bovine serum albumin (BSA) and 0.05 % saponin for 1 h at 4 °C. Oocytes were then incubated 2 h at 4 °C with

rabbit monoclonal anti-HA peptide (dilution 1:1,600; Cell Signaling, Danvers, MA), followed by three washes with 1 % PBS–BSA. Oocytes were then incubated for 2 h with Cy3-conjugated secondary donkey anti-rabbit Ig (dilution 1:1,600; Jackson Immunochemicals, West Grove, PA) and again thoroughly washed in PBS–BSA. Oocytes were aligned in uniform orientation along a plexiglass groove and sequentially imaged through the 10× objective of a Zeiss LSM510 laser scanning confocal microscope, using the 543-nm laser line at 512×512 resolution, at constant filter, gain, and pinhole settings.

Polypeptide abundance at or near each oocyte surface was estimated by quantitation of specific fluorescence intensity (FI) at the periphery of one quadrant of an equatorial focal plane (Image J v. 1.38, National Institutes of Health). The mean background FI of uninjected oocytes was subtracted from each single oocyte FI. Normalized means and standard errors were calculated for each group. Images of median intensity were selected from each group for presentation.

Statistics

Data are reported as mean±SEM. Flux data were compared by Student's paired *t*-test, or as appropriate by ANOVA with Dunnett's pairwise multiple comparison or Tukey's post-hoc analysis (SigmaPlot 11.0). A p value <0.05 was interpreted as significant.

Results

Missense substitution of all transmembrane domain cysteine residues of mAE2 preserves DIDS-sensitive Cl^-/Cl^- exchange activity

The mAE2 transmembrane domain (defined to encompass the short cytoplasmic C-terminal tail of the protein) includes eight Cys residues (Fig. 1a), only three of which are conserved in hAE1 (Fig. 1b). To prepare a construct useful for future Cys-insertion structure–function studies, all eight Cys residues were mutated as described in the Methods section and Table S1. *Xenopus* oocytes expressing $mAE2_{Cys\text{-}less}$ retained the ability to mediate Cl^- uptake sensitive to inhibition by DIDS (Fig. 2a), although at rates lower than exhibited by comparable oocytes injected with wildtype mAE2 cRNA. The Cl^- uptake by oocytes expressing $mAE2_{Cys\text{-}less}$ represented Cl^-/Cl^- exchange, as evidenced by trans-anion-dependent $^{36}Cl^-$ efflux that was DIDS-sensitive (Fig. 2b,c). $mAE2_{Cys\text{-}less(7/8)}$ also retained these activities (data not shown).

Anion exchange by $mAE2_{Cys\text{-}less}$ did not require the presence of the AE2 N-terminal cytoplasmic domain, as illustrated by $^{36}Cl^-$ uptake into oocytes expressing $mAE2_{Cys\text{-}less}$ Δ_N659 (Fig. 2d) and found previously for mAE2 [43]. Absence of the N-terminal cytoplasmic domain diminished the difference in influx between polypeptides containing and lacking transmembrane domain Cys residues. $mAE2_{Cys\text{-}less}$ was expressed at or near the oocyte surface with near-normal abundance (Fig. 3), suggesting the possibility that the observed reduced transport activity might in part represent decreased turnover number for Cl^-/Cl^- exchange, rather than decreased surface abundance alone.

Missense substitution of mAE2 transmembrane domain Cys residues maintains the $K_{1/2}$ for extracellular Cl^- of Cl^-/Cl^- exchange

The mAE2-mediated unidirectional influx of $^{36}Cl^-$ exhibited a $K_{1/2}$ value for extracellular [Cl^-] of 5.6 mM [22]. To measure $K_{1/2}$ based on efflux, we assessed the extracellular [Cl^-] dependence of the $^{36}Cl^-$ efflux rate constant in individual mAE2-expressing oocytes, and found it to be 5.5±0.9 mm (n=15; Fig. 4a). This value was indistinguishable whether derived from a fit to data from all oocytes or as the mean of fits to single oocyte efflux data. $mAE2_{Cys\text{-}less}$-mediated $^{36}Cl^-/Cl^-$ exchange exhibited a $K_{1/2}$ for extracellular [Cl^-] of 3.7+0.9 mM (n=9; p=0.53 vs. mAE2; Fig. 4b). Thus, the absence of transmembrane domain Cys residues does not change the apparent extracellular Cl^- affinity of mAE2.

Missense substitution of mAE2 transmembrane domain Cys residues preserves pH_i sensitivity but alkaline-shifts pH_o sensitivity of Cl^-/Cl^- exchange activity

DIDS-sensitive Cl^-/Cl^- exchange by mAE2-expressing *Xenopus* oocytes is inhibited by intracellular acidification to pH_i ~6.7 by replacement of pre-equilibrated 40 mM butyrate with impermeant anion [44]. This property of anion exchange inhibition by acidic intracellular pH is maintained in the absence of transmembrane domain Cys residues (Fig. 5a,b). Extracellular acidification independently inhibits mAE2 (Fig. 5c) in the presence of minimal [43] or no intracellular acidification [44]. Comparison of this inhibition in oocytes expressing mAE2 or $mAE2_{Cys\text{-}less}$ revealed an alkaline-shifted $pH_{o(50)}$ value for inhibition by extracellular protons in the absence of transmembrane domain Cys residues, from pH 6.85±0.06 (n=14) for mAE2 to a minimum value of pH 7.56±0.13 for $mAE2_{Cys\text{-}less}$ (Fig. 5d; calculated from individual oocyte pH_o vs. activity curves). The mean values calculated from individual oocye $pH_{o(50)}$ values differed to a similar degree, 6.94±0.04 for mAE2 and at least 7.47±0.08 for $mAE2_{Cys\text{-}less}$ (p<0.001). The true $pH_{o(50)}$ value for $mAE2_{Cys\text{-}less}$ may be higher than these estimates, since the normalized pH vs. activity curves did not reach definitive plateau values.

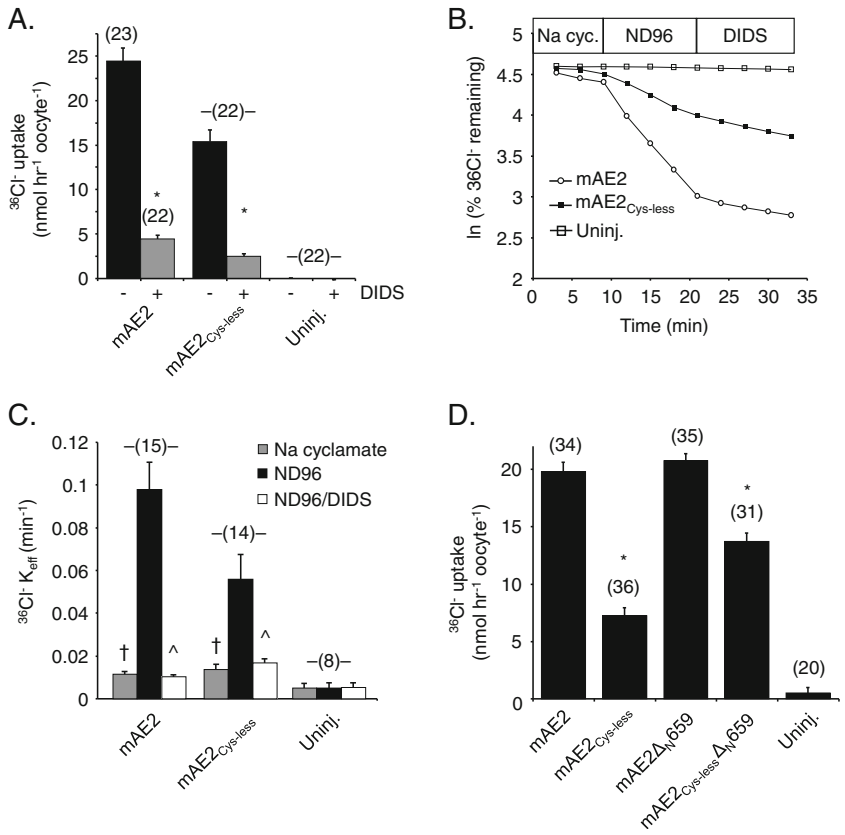

Fig. 2 Transmembrane domain cysteines are not essential for mAE2-mediated, DIDS-sensitive Cl^-/Cl^- exchange. **a** $^{36}Cl^-$ influx in the absence (−) or presence (+) of 500 μM DIDS was measured in uninjected oocytes (*Uninj.*) or in oocytes previously injected with 10 ng cRNA encoding wildtype mAE2 or $mAE2_{Cys\text{-}less}$. Values are means± SEM for (*n*) oocytes. *$p<0.05$ vs. absence of DIDS. Similar results were observed in another experiment 34 additional oocytes (not shown). **b** Representative $^{36}Cl^-$ efflux traces of individual oocytes into sequential baths of Na cyclamate (*Nacyc*), NaCl (ND96) and ND96+ 500 μM DIDS (DIDS). **c** $^{36}Cl^-$ efflux rate constants of (n) uninjected oocytes or oocytes previously injected with 10 ng of cRNA encoding mAE2 or $mAE2_{Cys\text{-}less}$, and subjected to the sequential bath changes of panel **b**. *$p<0.05$ vs. mAE2; ^$p<0.05$ vs. absence of DIDS; †$p<0.05$ vs. presence of Cl^-. **d** Cl^- transport by $mAE2_{Cys\text{-}less}$ does not require the AE2 N-terminal cytoplasmic domain. $^{36}Cl^-$ influx into (*n*) uninjected oocytes or oocytes previously injected with 10 ng of cRNA encoding mAE2, $mAE2_{Cys\text{-}less}$, mAE2 Δ_N659, or $mAE2_{Cys\text{-}less}$ Δ_N659. *$p<0.05$ vs. corresponding Cys-replete polypeptides

Missense substitution of mAE2 transmembrane domain Cys residues preserves stimulation of AE2-mediated Cl^-/Cl^- exchange activity by hypertonicity and by NH_4^+

mAE2-mediated Cl^-/Cl^- exchange activity in *Xenopus* oocytes is activated by bath hypertonicity [23], which slightly alkalinizes oocyte pH_i through activation of endogenous NHE1-like activity [17]. Exposure of oocytes expressing $mAE2_{Cys\text{-}less}$ exhibited similar activation by an increase in nominal bath tonicity from an isotonic value of 212–280 mOsm, and with further increased activity in the presence of 400 mOsm bath (Fig. 6a).

mAE2-mediated Cl^-/Cl^- exchange activity also exhibits unusual activation by addition of bath NH_4Cl, despite the atypical intracellular acidification produced in *Xenopus* oocytes by extracellular NH_4^+ addition [21]. As shown in Fig. 6b, $mAE2_{Cys\text{-}less}$ preserves this ability to respond to the acidifying stimulus of extracellular NH_4^+ addition with activation of Cl^-/Cl^- exchange.

Missense substitution of mAE2 transmembrane domain Cys residues preserves reversed pH sensitivity of SO_4^{2-} transport by the E1007Q mutant of AE2

Human erythrocytes exhibit AE1-mediated H^+/SO_4^{2-} co-transport in exchange for Cl^- [33]. Human AE1 E681 [25] and the corresponding mouse AE1 E699 [8] are critical residues for this and other anion exchange modes. The mAE1 E699Q mutation also reverses the normal stimulation of SO_4^{2-} transport by extracellular protons, such that SO_4^{2-} transport is stimulated by alkaline pH_o rather than by acidic pH_o [9].

The pH dependence of SO_4^{2-} transport by plasmalemmal AE2 in *Xenopus* oocytes has not been reported. Figure 7a shows that acidic pH_o indeed activates mAE2-mediated SO_4^{2-} uptake, as was previously shown for SO_4^{2-} transport by AE2 in HEK-293 cells [40] and with AE1-mediated transport of SO_4^{2-} in oocytes [9]. $mAE2_{Cys\text{-}less}$ exhibits ~4-fold lower rates of SO_4^{2-} transport but preserves some stimulation by

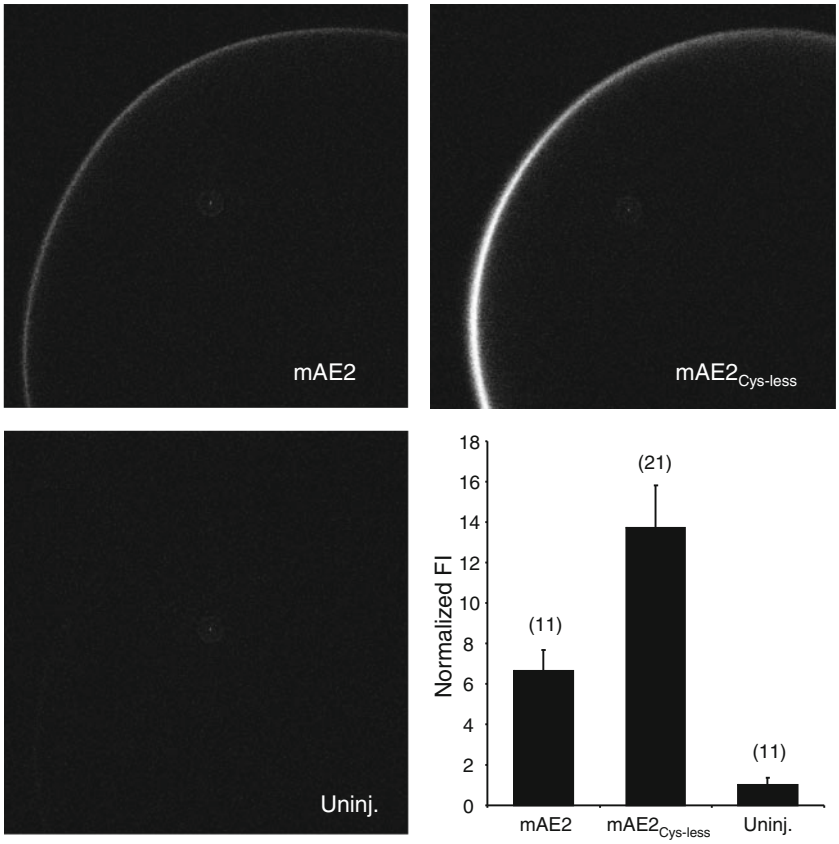

Fig. 3 Absence of transmembrane domain cysteines does not prevent mAE2 expression at or near the oocyte surface. Representative median intensity confocal immunofluorescence images of uninjected oocytes or oocytes previously injected with cRNA encoding mAE2 (20 ng) or $mAE2_{Cys\text{-}less}$ (50 ng). The *lower right panel* shows mean normalized fluorescence intensities for (*n*) oocytes ($p<0.05$ of each construct vs. uninjected oocytes (*uninj*.)

acidic pH_o. Introduction into mAE2 of the missense mutation E1007Q, corresponding to mAE1 E699Q, reverses pH_o dependence of AE2-mediated SO_4^{2-} transport such that alkaline pH_o stimulates it. The absence of transmembrane domain Cys residues similarly decreases SO_4^{2-} transport rates by mAE2 E1007Q, but preserves the "reversed" stimulation by alkaline pH_o (Fig. 7a).

AE1-mediated oxalate transport in erythrocytes is also activated by extracellular protons, consistent with a mechanism of H^+/oxalate vs. Cl^- exchange [26]. Figure 7b shows that mAE2-mediated oxalate uptake is also strongly stimulated by acidic pH_o. However, although oxalate uptake by $mAE2_{Cys\text{-}less}$-expressing oocytes was proportionately reduced to the same degree as was SO_4^{2-} uptake by mAE2 (Fig. 7a), activation of oxalate uptake by acidic pH_o was not evident in oocytes expressing $mAE2_{Cys\text{-}less}$.

Missense substitutions at mAE2 E1007 produce less severe impairment of Cl^- transport than do corresponding substitutions at mAE1 E699, but loss-of-function is exacerbated by absence of AE2 transmembrane domain Cys residues.

Xenopus oocytes expressing mAE1 E699Q or any of several other missense substitutions at the same position exhibited complete loss of Cl^- transport, strengthening the contention that E699 constitutes part of the AE1 anion translocation pathway [8]. Figure 8 shows that the corresponding mAE2 missense mutation E1007Q produced less than complete loss of Cl^- transport function that can be partially overcome by increasing the mass of injected cRNA. We therefore tested the effect of other substitutions at residue 1007. Substitution of Cys or His also produced less than complete loss of Cl^- transport, again partially overcome by increasing the mass of injected cRNA. mAE2 E1007K exhibited the greatest loss of Cl^- transport function. Absence of AE2 transmembrane domain Cys residues exacerbated the reduced Cl^- influx phenotype of each E1007 substitution tested (Fig. 8).

Discussion

In this work we have shown that DIDS-sensitive Cl^-/Cl^- exchange mediated by $mAE2_{Cys\text{-}less}$ retained nearly all native regulatory properties of wildtype mAE2, but with three notable differences. First, in the absence of transmembrane domain Cys residues the AE2-mediated Cl^-/Cl^- exchange rate was reduced ~50 %, in the context of near-normal polypeptide surface abundance. Second, although both wildtype AE2 and $AE2_{Cys\text{-}less}$ were inhibited by acidic intracellular pH, the $pHo_{(50)}$ value of $mAE2_{Cys\text{-}less}$ for inhibition by extracellular protons was alkaline-shifted >0.6–0.7 pH units. Third, activation of mAE2-mediated oxalate transport by acidic pH_o was abolished in $mAE2_{Cys\text{-}less}$.

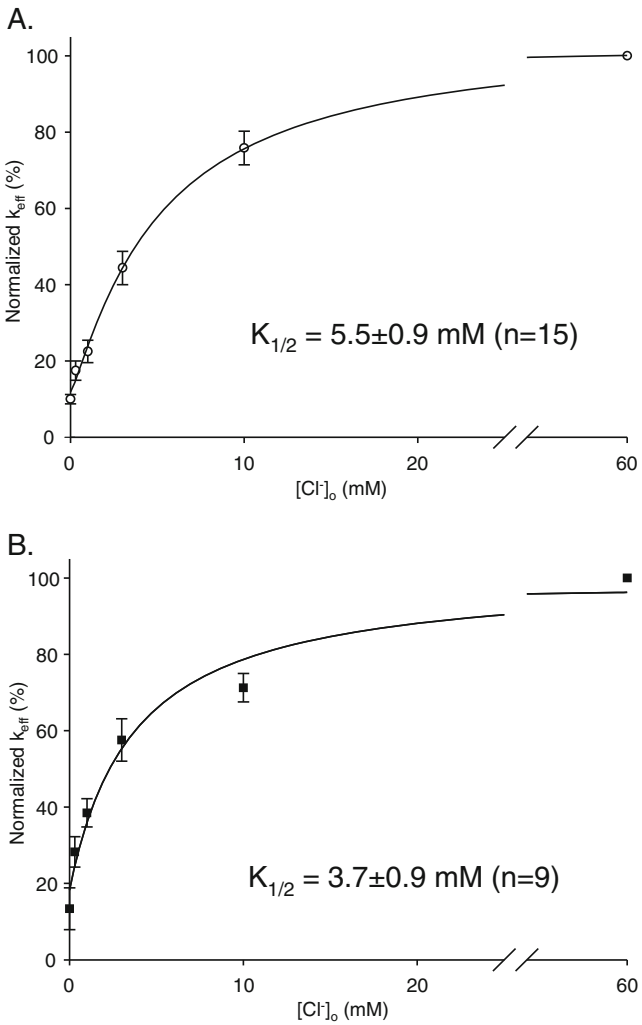

Fig. 4 $K_{1/2}(Cl^-_o)$ of mAE2-mediated $^{36}Cl^-$ efflux is minimally affected by absence of transmembrane domain Cys residues. **a** Extracellular $[Cl^-]$-dependence of normalized rate constants of mAE2-mediated $^{36}Cl^-$ efflux (n=15, oocytes previously injected with 2 ng cRNA). **b** Extracellular $[Cl^-]$-dependence of normalized rate constants of $mAE2_{Cys\text{-}less}$-mediated $^{36}Cl^-$ efflux (n=11, oocytes previously injected with 10 ng cRNA). Na cyclamate was substituted mole for mole by NaCl to achieve bath $[Cl^-]$ of 0.3, 1, 3, 10 and 60 mM. Mean $^{36}Cl^-$ efflux rate constants of uninjected oocytes (n=5) were subtracted from efflux rate constants of each groups, and data was fit as described in Methods. The $K_{1/2}$ values did not differ between groups (p=0.53)

Effects of Cysteine substitution on membrane transport proteins

The prototype for cysteine scanning mutagenesis studies as "an approach to membrane transport protein structure without crystals" has been the LacY H^+/lactate cotransporter of *Escherichia. coli* [14, 41]. After demonstration that Cys residues are not essential to LacY transport function, Cys substitution was applied to nearly every residue of Cys-less LacY. Investigation of these mutants through a range of biochemical and biophysical approaches has yielded an extensive set of results consistent with insights available from crystal structures [1, 7].

With a similar approach to the study of hAE1 in mind, Casey et al. substituted all five Cys residues of hAE1 (three in the transmembrane domain) with serine residues [6]. At that time, the role of cysteine residues in AE1 function remained unclear. Previous studies in human red cells had shown hAE1 to be stably palmitoylated on C843 [36], but mutation of the corresponding C841 in mAE1 to Ser or Met did not impair stilbene-sensitive anion exchange in *Xenopus* oocytes [27]. Moreover, C843 was not palmitoylated in heterologous hAE1 overexpressed in HEK293 or COS7 cells. Indeed, in these cell types, overexpressed hAE1 C843A underwent apparently normal *N*-glycosylation and trafficked normally to the cell surface [11].

More recently, combined distal renal tubular acidosis and hereditary spherocytosis was shown to be associated with the hAE1 missense substitution C479W, in compound heterozygosity with recessive mutation G701D. The mutant C479W polypeptide was retained in the endoplasmic reticulum of polarized MDCK cells, and contributed to reduced AE1 abundance in red cells [12]. Mutations to Cys of hAE1 residues R490, R518, and R808 also cause hereditary spherocytosis. In addition, the hAE1 mutation R730C causes stomatocytosis [45], and hAE1 mutation R589C causes distal renal tubular acidosis [42]. hAE1 Cys residues 201 and 317 of the cytoplasmic domain and Cys 843 of the transmembrane domain have (more speculatively) also been proposed to provide red cell efflux shuttle pathways for selenious acid and for nitric oxide [20], pathways of undefined relationship to the anion translocation pathway utilized by the anion exchange mechanism.

Cys-less AE1 retained about half of wildtype Cl^-/HCO_3^- exchange activity when expressed in HEK-293 cells, but normalization of activity to surface abundance suggested that exchange turnover number was unchanged in the absence of AE1 Cys residues [6, 49]. In contrast, Cl^-/HCO_3^- exchange activity in *Xenopus* oocytes expressing Cys-less hAE1 was later reported to be undetectable due to surface expression below the detection threshold [5]. More dramatically still, missense substitution of all seven Cys residues of the trout AE1 transmembrane domain led to absence of detectable tAE1 polypeptide in cRNA-injected oocytes, with consequent loss of tAE1-mediated Cl^- conductance [30]. Mutation of the single C462 of tAE1 sufficed to lead to intracellular retention of polypeptide, similar to the phenotype of the corresponding dRTA mutation C479W of hAE1. Moreover, two single-Cys mutants of tAE1 (in positions at which mammalian AE1 lacks Cys residues) exhibited proportionately greater loss of the tAE1-associated Cl^- conductance than of Cl^-/HCO_3^- exchange [30].

SLC4A4/NBCe1 was shown to be an ecto-disulfide-linked dimer [28], very much unlike the noncovalent SLC4 family homodimers, AE1 and AE2. Cys scan mutations of SLC4A4/NBC31 have not been performed in

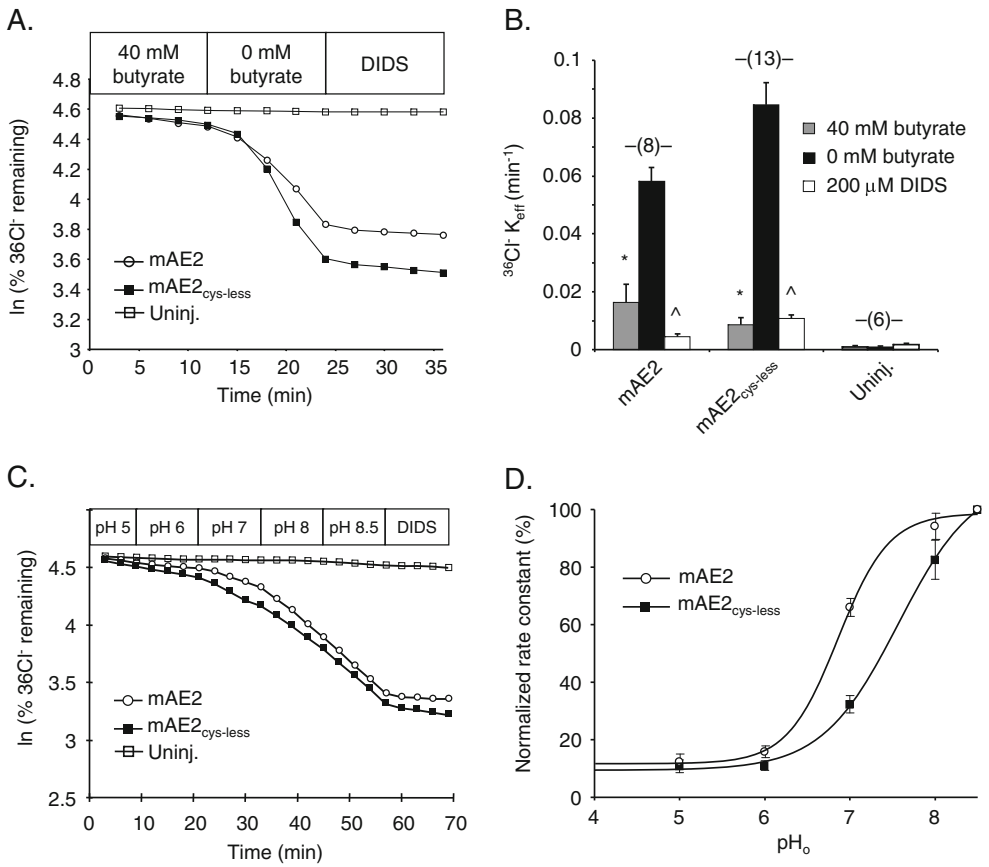

Fig. 5 Absence of transmembrane domain cysteines does not grossly alter mAE2 pH_i sensitivity, but shifts mAE2 pH_o sensitivity curve to more alkaline pH values. **a** $^{36}Cl^-$ efflux traces from representative individual oocytes previously uninjected (*open squares*) or injected with cRNA encoding mAE2 (1 ng; *open circles*) or $mAE2_{Cys\text{-}less}$ (10 ng; *filled squares*), and subjected to sequential exposure to baths containing ND-56 plus 40 mM Na butyrate, then ND-56 plus 40 mM Na cyclamate (0 butyrate), then ND-56 plus 40 mM Na cyclamate with added 200 μM DIDS (*DIDS*). **b** Mean $^{36}Cl^-$ efflux rate constants of (*n*) oocytes subjected to the experimental conditions in panel **a**. *,^ $p<0.05$ vs. cyclamate (0 butyrate). Values are means±SEM. **c** $^{36}Cl^-$ efflux traces from representative individual oocytes previously uninjected (*open squares*) or injected with cRNA encoding mAE2 (1 ng; *open circles*) or $mAE2_{Cys\text{-}less}$ (10 ng; *filled squares*), and subjected to sequential exposure to baths containing ND-96 at the indicated pH values, followed by exposure to 200 μM DIDS (*DIDS*). **d** Mean normalized $^{36}Cl^-$ efflux rate constants (±SEM) of oocytes previously injected with cRNA encoding mAE2 WT (0.5–2 ng, $n=14$) or $mAE2_{Cys\text{-}less}$ (5–20 ng, $n=23$) as a function of bath pH values, measured as in panel **c**. All values reflect subtraction of the mean $^{36}Cl^-$ efflux rate constant of uninjected oocytes measured during the same experiments ($n=9$). Mean $pH_{o(50)}$ values were 6.94 for mAE2 and a minimum value of 7.47 for $mAE2_{Cys\text{-}less}$ ($p<0.001$). (Note that the $mAE2_{Cys\text{-}less}$ pH_o vs. activity curve did not reach a definitive plateau)

oocytes, but that performed in HEK-293 cells has predicted a structure for the C-terminal half of the NBCe1 transmembrane domain quite different from that of AE1 [61]. The functional capacity of Cys-less SLC4A4/NBCe1 has not been reported, although the Cys-less polypeptide has been expressed. SLC4A4/NBCe1 was functional in the absence of five of its 15 Cys residues (five of its 12 transmembrane domain Cys residues as defined as in this paper on AE2), but rates were not directly compared to those of wildtype NBCe1 [62]. The above results for Cys substitution and Cys scan experiments in NBCe1 show that results obtained with one SLC4 protein cannot necessarily be extrapolated with confidence to another SLC4 protein, even when closely related.

Indeed, the functional importance of transmembrane domain Cys residues can vary according to gene product, species of origin, and expression system. For example, whereas engineered removal of all Cys residues from nucleobase transporter hENT1 led to complete loss-of-function [53], Cys-less forms of glucose transporter GLUT1 [34], organic cation transporter MATE1 [55], glutamate transporter EAAT1 [39], and the H^+-coupled folate transporter [57] retained all or nearly all functional activity. More subtle phenotypes of Cys-less proteins as compared to their corresponding wildtype polypeptides included decreased plasmalemmal trafficking and single channel conductance in Cys-less CFTR [19], loss of 5-fluoro-maleimide inhibition of otherwise intact channel activity of Cys-less mitochondrial porin VDAC [4], and increased susceptibility to loss-of-function by otherwise inactive second-site mutations in the H^+-coupled folate transporter [57].

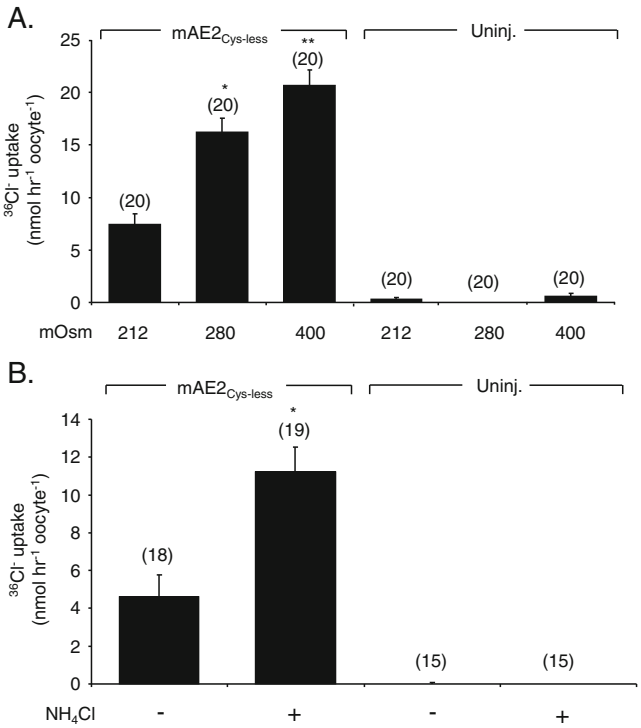

Fig. 6 Absence of transmembrane domain cysteines does not grossly alter mAE2 activation by hypertonicity or by NH_4^+. **a** $^{36}Cl^-$ influx into (*n*) uninjected oocytes or oocytes previously injected with 10 ng of cRNA encoding $mAE2_{Cys\text{-}less}$ in bath solutions of indicated osmolarity. ND-96 osmolarity is 212 mOsm. *$p<0.05$ vs. 212 mOsm; **$p<0.05$ vs. 212 or 280 mOsm. **b** $^{36}Cl^-$ influx into (*n*) uninjected oocytes or oocytes previously injected with 10 ng of cRNA encoding $mAE2_{Cys\text{-}less}$ in baths of ND96 (−) or ND-70 plus 26 mM NH_4Cl (+). *$p<0.001$ vs. ND-96. Values are means ± SEM

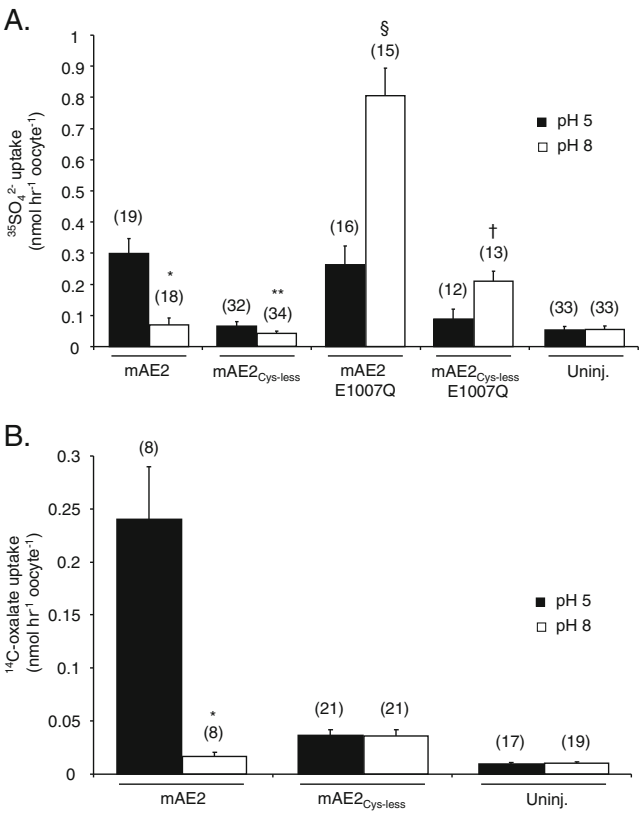

Fig. 7 Absence of mAE2 transmembrane domain cysteines does not prevent acidic pH_o activation of SO_4^{2-} transport by mAE2 E1007Q, but abolishes H^+-stimulated oxalate transport by mAE2. **a** $^{35}SO_4^{2-}$ influx into (*n*) uninjected oocytes or oocytes previously injected with 50 ng cRNA encoding mAE2 or $mAE2_{Cys\text{-}less}$ without or with the missense substitution mutation E1007Q, measured in baths of pH 5.0 (*black bars*) or 8.0 (*white bars*). *$p<0.001$ vs. pH 5; = **$p<0.005$ vs. pH 5; §$p<0.001$ vs. pH 5; †$p<0.01$ vs. pH 5. **b** ^{14}C oxalate influx into (*n*) uninjected oocytes or oocytes previously injected with 50 ng cRNA encoding mAE2 or $mAE2_{Cys\text{-}less}$. *$p<0.001$ vs. pH 5. Values are means ± SEM

Absence of transmembrane Cys residues preserves many normal functions of mAE2

The absence of transmembrane domain Cys residues decreases rates of AE2-mediated Cl^-/Cl^- exchange in *Xenopus* oocytes from 40 % to 75 % (Fig. 2), in the context of near-normal polypeptide surface abundance (Fig. 3). The removal from $mAE2_{Cys\text{-}less}$ of most of its N-terminal cytoplasmic domain does not further decrease transport activity, and may even stimulate it (Fig. 3). The apparent affinity of AE2 for extracellular Cl^- is not significantly altered in the absence or transmembrane Cys residues (Fig. 4). The ability of AE2 to be activated by hypertonicity or by isotonic NH_4Cl is also preserved in the absence of transmembrane domain Cys residues (Fig. 6). In addition, the inhibition of AE2 by intracellular protons and removal of inhibition during recovery from intracellular acidosis (by exposure to and withdrawal from bath butyrate) is preserved apparently intact in the absence of transmembrane domain Cys residues (Fig. 5a,b). The integrity of these regulatory properties in $mAE2_{Cys\text{-}less}$ suggests that transmembrane domain Cys substitution does not result in large-scale conformational change.

AE2 sensitivity to pH_o is altered by absence of transmembrane domain cysteines

The $pH_{o(50)}$ value of $mAE2_{Cys\text{-}less}$ is at least 0.6–0.7 pH units higher than that of mAE2 (Fig. 5c,d). The absence of the first 199 N-terminal amino acids encoded by the naturally occurring variant transcript AE2c1, abundantly expressed only in gastric mucosa, produces an alkaline shift of comparable magnitude in the $pH_{o(50)}$ of mAE2 [29]. The physiological rationale for expression of the Ae2c1 transcript may be to extend the extracellular (interstitial space) pH range across which gastric parietal cell AE2 remains fully active during the alkaline tide generated during maximal stimulation of lumenal H^+ secretion. However, the mechanism by which both absence of the first 199 N-terminal amino acids of AE2a and absence of transmembrane domain Cys residues increase the apparent affinity of extracellular proton-associated inhibition of AE2-mediated

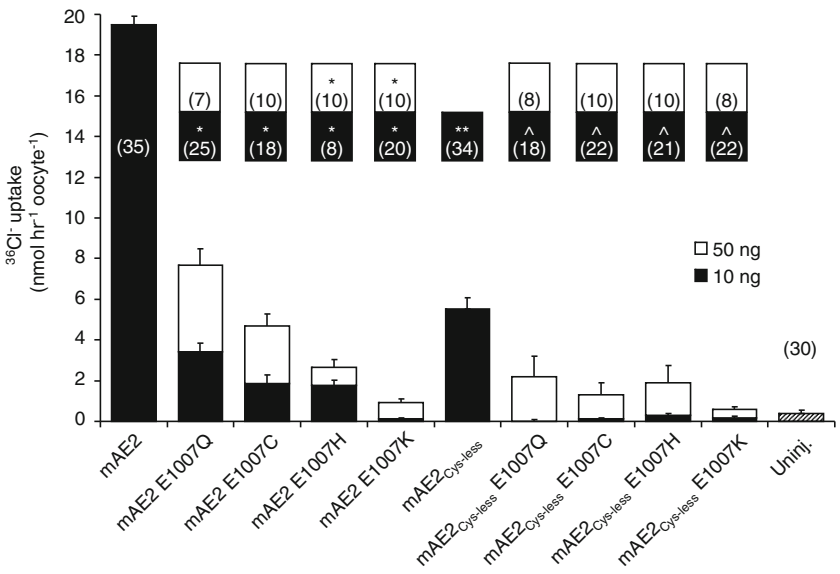

Fig. 8 Substitution mutations at mAE2 E1007 produce partial loss of Cl^- transport, exacerbated by absence of transmembrane domain Cys residues. Role in $^{36}Cl^-$ influx of amino acid substitutions at mAE2a position E1007 in (*n*) oocytes previously injected with 10 ng (*black bars*) or 50 ng (*white bars*) of mAE2 or $mAE2_{Cys\text{-}less}$ cRNAs, or their indicated E1007 missense substitution mutants. $^{36}Cl^-$ influx into uninjected oocytes is indicated by the hatched bar at the far right. Values are means ± SEM. *$p<0.05$ vs. mAE2 10 ng; **$p<0.001$ vs. mAE2 10 ng; ^$p<0.05$ vs. $mAE2_{Cys\text{-}less}$ 10 ng

anion exchange activity remains obscure, and the structure of neither AE2 region is known. The slow onset and progression of AE2-deficiency phenotypes in $AE2^{a,b-/-}$ mice [24, 32, 37, 38] compared to the complete AE2 knockout [16] suggests compensatory ectopic expression of AE2c1 that prevents the perinatal death associated with complete AE2 deficiency [16]. The alkaline-shifted pH_o sensitivity of AE2c1 in these processes has not been examined. (See Fig. 1a of ref. 28 for a comparison of the N-terminal amino acid sequences of the five variant transcripts of mAE2.)

Missense mutations on either intracellular or extracellular faces of AE2 can regulate anion transport sensitivity to both *cis* and *trans* protons, suggesting conformational responses in both domains in response to changes in pH that extend beyond the site of substitution [46, 48]. In particular, mAE2 $pH_{o(50)}$ was alkaline-shifted to 7.6 in the mAE2 mutant I1079C, located in the first re-entrant loop of the transmembrane domain [47]. In addition, mAE2 $pH_{o(50)}$ values were slightly alkaline-shifted to ~7.2 in mutants K889A, H1144A, H1145A, and double mutants H1144/H1145 and A1041/A1053 [46, 48]. The mechanistic relationship between the alkaline-shifted $pH_{o(50)}$ caused by these mutations and that caused by complete transmembrane domain Cys substitution remains unknown.

Absence of transmembrane domain Cys residues differentially alters regulation of SO_4^{2-} and oxalate exchange by pH_o

The effect of the absence of transmembrane Cys residues on the pH sensitivity of Cl^- transport led us to examine the effects on pH-sensitive transport of divalent anions. We showed previously that the mAE1-mediated electroneutral exchange of Cl^- for the H^+/SO_4^{2-} ion pair, activated by acidic pH_o, is converted by the mAE1 E699Q mutation to electrogenic SO_4^{2-}/Cl^- exchange [8] activated by alkaline pH_o [9]. Activation by acidic pH_o of AE2-mediated SO_4^{2-} uptake was preserved in the absence of transmembrane domain Cys residues, as was activation by alkaline pH_o of AE2 E1007Q-mediated SO_4^{2-} uptake (Fig. 7a). The absence of transmembrane domain cysteines exacerbated reduction in transport function by all E1007 missense substitutions tested for mAE2 (Fig. 8). In addition to reducing the rate of oxalate transport, the absence of transmembrane domain cysteines also resulted in loss of activation by acidic pH_o of AE2-mediated oxalate uptake (Fig. 7b). The reasons for the differing responses of pH-sensitive transport of SO_4^{2-} and oxalate are not clear, but may relate to ionic radius and/or to variable oxalate geometry in free and liganded states [13].

It is of interest to note that mAE2 mutation E1007Q exhibits a less severe oocyte Cl^- transport phenotype (Fig. 8) than does the corresponding mAE1 E699Q mutant [8]. However, other missense substitutions at mAE2 E1007 exhibit total loss of Cl^- transport, suggesting that this Glu residue is very likely situated along the anion translocation pathway in both AE1 and AE2. mAE1 E699 and mAE2 E1007 are believed to reside at or near the cytoplasmic end of transmembrane helix 8. The less severe mAE2 phenotype may reflect local differences in their steric and electrostatic environments, as depicted in Fig. S1. mAE2 E1007 is bracketed by M1006 and T1008, whereas hAE1 E681 is bracketed by L680 and S682. (This region of mAE1 is identical in amino acid sequence.) Integration of these sequence differences into a context of neighboring transmembrane helices and intracellular loops remains elusive, due to the inadequately resolved transmembrane domain structure of any SLC4 polypeptide.

Prospects

The availability of $mAE2_{Cys\text{-}less}$ will allow directed cysteine scanning mutagenesis throughout the AE2 transmembrane domain in the absence of endogenous Cys residues. Such

single Cys insertions will be important to test the predictive utility of electron microscopic and crystal structures of increasing resolution. Most regulatory properties of $AE2_{Cys\text{-}less}$ will be amenable to study in this fashion, including the inhibitory regulation by intracellular protons. However, the inhibitory regulation of AE2 by extracellular protons is alkali-shifted by the absence of transmembrane domain Cys residues. Targeted reintroduction of individual or multiple native Cys residues may identify those of greatest importance in setting $pH_{o(50)}$ of mAe2. In the meantime, this difference in regulation will need to be taken into account when interpreting the results of single Cys substitutions in the $AE2_{Cys\text{-}less}$ background. An understanding of the similarly shifted $pH_{o(50)}$ values of AE2c1 and $AE2_{Cys\text{-}less}$ may emerge from atomic-level resolution structures of AE1 or another member of the SLC4 superfamily. Such understanding should serve to enhance models of cellular homeostasis that balance the sometimes conflicting demands on Cl^- transport in the service of regulating intracellular and systemic pH and in volume regulation.

Acknowledgments We thank Dr. David H. Vandorpe of Beth Israel Deaconess Medical Center and Harvard Medical School for helpful discussion. This work was supported by a Robert Bosch Foundation fellowship to FRR, by a University of Copenhagen stipend to KS, and by NIH grants DK43495 and DK34854 (The Harvard Digestive Diseases Center) to SLA.

Ethical standards The experiments presented in this paper conform to the laws of the USA, where they were performed.

Conflict of interest The authors declare that they have no conflict of interest.

References

1. Abramson J, Smirnova I, Kasho V, Verner G, Kaback HR, Iwata S (2003) Structure and mechanism of the lactose permease of *Escherichia coli*. Science (New York NY) 301:610–615
2. Alper SL (2009) Molecular physiology and genetics of Na^+-independent SLC4 anion exchangers. J Exp Biol 212:1672–1683
3. Alper SL (2010) Familial renal tubular acidosis. J Nephrol 23 (Suppl 16):S57–S76
4. Aram L, Geula S, Arbel N, Shoshan-Barmatz V (2010) VDAC1 cysteine residues: topology and function in channel activity and apoptosis. Biochem J 427:445–454
5. Barneaud-Rocca D, Borgese F, Guizouarn H (2011) Dual transport properties of anion exchanger 1: the same transmembrane segment is involved in anion exchange and in a cation leak. J Biol Chem 286:8909–8916
6. Casey JR, Ding Y, Kopito RR (1995) The role of cysteine residues in the erythrocyte plasma membrane anion exchange protein, AE1. J Biol Chem 270:8521–8527
7. Chaptal V, Kwon S, Sawaya MR, Guan L, Kaback HR, Abramson J (2011) Crystal structure of lactose permease in complex with an affinity inactivator yields unique insight into sugar recognition. Proc Natl Acad Sci U S A 108:9361–9366
8. Chernova MN, Jiang L, Crest M, Hand M, Vandorpe DH, Strange K, Alper SL (1997) Electrogenic sulfate/chloride exchange in Xenopus oocytes mediated by murine AE1 E699Q. J Gen Physiol 109:345–360
9. Chernova MN, Stewart AK, Barry PN, Jennings ML, Alper SL (2008) Mouse Ae1 E699Q mediates $SO_4^{2-}$$_i$/anion$_o$ exchange with $[SO_4^{2-}]_i$-dependent reversal of wild-type pH_o sensitivity. Am J Physiol 295:C302–C312
10. Chernova MN, Stewart AK, Jiang L, Friedman DJ, Kunes YZ, Alper SL (2003) Structure–function relationships of AE2 regulation by Ca(i)(2+)-sensitive stimulators NH(4+) and hypertonicity. Am J Physiol 284:C1235–C1246
11. Cheung JC, Reithmeier RA (2004) Palmitoylation is not required for trafficking of human anion exchanger 1 to the cell surface. Biochem J 378:1015–1021
12. Chu C, Woods N, Sawasdee N, Guizouarn H, Pellissier B, Borgese F, Yenchitsomanus PT, Gowrishankar M, Cordat E (2010) Band 3 Edmonton I, a novel mutant of the anion exchanger 1 causing spherocytosis and distal renal tubular acidosis. Biochem J 426:379–388
13. Dean PA (2012) The oxalate dianion: planar or non-planar? J Chem Educ 89:417–418
14. Frillingos S, Sahin-Toth M, Wu J, Kaback HR (1998) Cys-scanning mutagenesis: a novel approach to structure function relationships in polytopic membrane proteins. FASEB J 12:1281–1299
15. Gawenis LR, Bradford EM, Alper SL, Prasad V, Shull GE (2010) AE2 Cl^-/HCO_3^- exchanger is required for normal cAMP-stimulated anion secretion in murine proximal colon. Am J Physiol Gastrointest Liver Physiol 298:G493–G503
16. Gawenis LR, Ledoussal C, Judd LM, Prasad V, Alper SL, Stuart-Tilley A, Woo AL, Grisham C, Sanford LP, Doetschman T, Miller ML, Shull GE (2004) Mice with a targeted disruption of the AE2 Cl^-/HCO_3^- exchanger are achlorhydric. J Biol Chem 279:30531–30539
17. Goss GG, Jiang L, Vandorpe DH, Kieller D, Chernova MN, Robertson M, Alper SL (2001) Role of JNK in hypertonic activation of Cl(−)-dependent Na(+)/H(+) exchange in Xenopus oocytes. Am J Physiol 281:C1978–C1990
18. Heneghan JF, Akhavein A, Salas MJ, Shmukler BE, Karniski LP, Vandorpe DH, Alper SL (2010) Regulated transport of sulfate and oxalate by SLC26A2/DTDST. Am J Physiol 298:C1363–C1375
19. Holstead RG, Li MS, Linsdell P (2011) Functional differences in pore properties between wild-type and cysteine-less forms of the CFTR chloride channel. J Membr Biol 243:15–23
20. Hongoh M, Haratake M, Fuchigami T, Nakayama M (2012) A thiol-mediated active membrane transport of selenium by erythroid anion exchanger 1 protein. Dalton Trans 41:7340–7349
21. Humphreys BD, Chernova MN, Jiang L, Zhang Y, Alper SL (1997) NH4Cl activates AE2 anion exchanger in Xenopus oocytes at acidic pH_i. Am J Physiol 272:C1232–C1240
22. Humphreys BD, Jiang L, Chernova MN, Alper SL (1994) Functional characterization and regulation by pH of murine AE2 anion exchanger expressed in Xenopus oocytes. Am J Physiol 267: C1295–C1307
23. Humphreys BD, Jiang L, Chernova MN, Alper SL (1995) Hypertonic activation of AE2 anion exchanger in Xenopus oocytes via NHE-mediated intracellular alkalinization. Am J Physiol 268:C201–C209
24. Jansen ID, Mardones P, Lecanda F, de Vries TJ, Recalde S, Hoeben KA, Schoenmaker T, Ravesloot JH, van Borren MM, van Eijden TM, Bronckers AL, Kellokumpu S, Medina JF, Everts V, Oude Elferink RP (2009) Ae2(a, b)-deficient mice exhibit osteopetrosis of long bones but not of calvaria. FASEB J 23:3470–3481
25. Jennings ML (1995) Rapid electrogenic sulfate-chloride exchange mediated by chemically modified band 3 in human erythrocytes. J Gen Physiol 105:21–47
26. Jennings ML, Adame MF (1996) Characterization of oxalate transport by the human erythrocyte band 3 protein. J Gen Physiol 107:145–159

27. Kang D, Karbach D, Passow H (1994) Anion transport function of mouse erythroid band 3 protein (AE1) does not require acylation of cysteine residue 861. Biochim Biophys Acta 1194:341–344
28. Kao L, Sassani P, Azimov R, Pushkin A, Abuladze N, Peti-Peterdi J, Liu W, Newman D, Kurtz I. J Biol Chem. 2008. 283:26782–26794
29. Kurschat CE, Shmukler BE, Jiang L, Wilhelm S, Kim EH, Chernova MN, Kinne RK, Stewart AK, Alper SL (2006) Alkaline-shifted pHo sensitivity of AE2c1-mediated anion exchange reveals novel regulatory determinants in the AE2 N-terminal cytoplasmic domain. J Biol Chem 281:1885–1896
30. Martial S, Guizouarn H, Gabillat N, Pellissier B, Borgese F (2007) Importance of several cysteine residues for the chloride conductance of trout anion exchanger 1 (tAE1). J Cell Physiol 213:70–78
31. McAlear SD, Bevensee MO (2006) A cysteine-scanning mutagenesis study of transmembrane domain 8 of the electrogenic sodium/bicarbonate cotransporter NBCe1. J Biol Chem 281:32417–32427
32. Medina JF, Recalde S, Prieto J, Lecanda J, Saez E, Funk CD, Vecino P, van Roon MA, Ottenhoff R, Bosma PJ, Bakker CT, Elferink RP (2003) Anion exchanger 2 is essential for spermiogenesis in mice. Proc Natl Acad Sci U S A 100:15847–15852
33. Milanick MA, Gunn RB (1984) Proton–sulfate cotransport: external proton activation of sulfate influx into human red blood cells. Am J Physiol 247:C247–C259
34. Mueckler M, Makepeace C (2009) Model of the exofacial substrate-binding site and helical folding of the human Glut1 glucose transporter based on scanning mutagenesis. Biochemistry 48:5934–5942
35. Muller-Berger S, Karbach D, Kang D, Aranibar N, Wood PG, Ruterjans H, Passow H (1995) Roles of histidine 752 and glutamate 699 in the pH dependence of mouse band 3 protein-mediated anion transport. Biochemistry 34:9325–9332
36. Okubo K, Hamasaki N, Hara K, Kageura M (1991) Palmitoylation of cysteine 69 from the COOH-terminal of band 3 protein in the human erythrocyte membrane. Acylation occurs in the middle of the consensus sequence of F–I-IICLAVL found in band 3 protein and G2 protein of Rift Valley fever virus. J Biol Chem 266:16420–16424
37. Recalde S, Muruzabal F, Looije N, Kunne C, Burrell MA, Saez E, Martinez-Anso E, Salas JT, Mardones P, Prieto J, Medina JF, Elferink RP (2006) Inefficient chronic activation of parietal cells in Ae2a, b(−/−) mice. Am J Pathol 169:165–176
38. Salas JT, Banales JM, Sarvide S, Recalde S, Ferrer A, Uriarte I, Oude Elferink RP, Prieto J, Medina JF (2008) Ae2a, b-deficient mice develop antimitochondrial antibodies and other features resembling primary biliary cirrhosis. Gastroenterology 134:1482–1493
39. Seal RP, Amara SG (1998) A reentrant loop domain in the glutamate carrier EAAT1 participates in substrate binding and translocation. Neuron 21:1487–1498
40. Sekler I, Lo RS, Kopito RR (1995) A conserved glutamate is responsible for ion selectivity and pH dependence of the mammalian anion exchangers AE1 and AE2. J Biol Chem 270:28751–28758
41. Smirnova I, Kasho V, Kaback HR (2011) Lactose permease and the alternating access mechanism. Biochemistry 50:9684–9693
42. Stewart AK, Alper, S.L. (2012) The SLC4 anion exchanger gene family. In: Alpern RJ, Hebert SC (ed) The Kidney: Pathophysiology and Pathophysiology. Elsevier, San Diego. Chapter 54. pp. 1857–1911
43. Stewart AK, Chernova MN, Kunes YZ, Alper SL (2001) Regulation of AE2 anion exchanger by intracellular pH: critical regions of the NH(2)-terminal cytoplasmic domain. Am J Physiol 281: C1344–C1354
44. Stewart AK, Chernova MN, Shmukler BE, Wilhelm S, Alper SL (2002) Regulation of AE2-mediated Cl^- transport by intracellular or by extracellular pH requires highly conserved amino acid residues of the AE2 NH2-terminal cytoplasmic domain. J Gen Physiol 120:707–722
45. Stewart AK, Kedar PS, Shmukler BE, Vandorpe DH, Hsu A, Glader B, Rivera A, Brugnara C, Alper SL (2011) Functional characterization and modified rescue of novel AE1 mutation R730C associated with overhydrated cation leak stomatocytosis. Am J Physiol 300:C1034–C1046
46. Stewart AK, Kurschat CE, Alper SL (2007) Role of nonconserved charged residues of the AE2 transmembrane domain in regulation of anion exchange by pH. Pflugers Arch 454:373–384
47. Stewart AK, Kurschat CE, Vaughan-Jones RD, Alper SL (2009) Putative re-entrant loop 1 of AE2 transmembrane domain has a major role in acute regulation of anion exchange by pH. J Biol Chem 284:6126–6139
48. Stewart AK, Kurschat CE, Vaughan-Jones RD, Shmukler BE, Alper SL (2007) Acute regulation of mouse AE2 anion exchanger requires isoform-specific amino acid residues from most of the transmembrane domain. J Physiol 584:59–73
49. Tang XB, Fujinaga J, Kopito R, Casey JR (1998) Topology of the region surrounding Glu681 of human AE1 protein, the erythrocyte anion exchanger. J Biol Chem 273:22545–22553
50. Taylor AM, Zhu Q, Casey JR (2001) Cysteine-directed cross-linking localizes regions of the human erythrocyte anion-exchange protein (AE1) relative to the dimeric interface. Biochem J 359:661–668
51. Wu J, Glimcher LH, Aliprantis AO (2008) HCO_3^-/Cl^- anion exchanger SLC4A2 is required for proper osteoclast differentiation and function. Proc Natl Acad Sci U S A 105:16934–16939
52. Yamaguchi T, Ikeda Y, Abe Y, Kuma H, Kang D, Hamasaki N, Hirai T (2010) Structure of the membrane domain of human erythrocyte anion exchanger 1 revealed by electron crystallography. J Mol Biol 397:179–189
53. Yao SY, Ng AM, Cass CE, Baldwin SA, Young JD (2011) Nucleobase transport by human equilibrative nucleoside transporter 1 (hENT1). J Biol Chem 286:32552–32562
54. Zhang D, Kiyatkin A, Bolin JT, Low PS (2000) Crystallographic structure and functional interpretation of the cytoplasmic domain of erythrocyte membrane band 3. Blood 96:2925–2933
55. Zhang X, Wright SH (2009) MATE1 has an external COOH terminus, consistent with a 13-helix topology. Am J Physiol Renal Physiol 297:F263–F271
56. Zhang Y, Chernova MN, Stuart-Tilley AK, Jiang L, Alper SL (1996) The cytoplasmic and transmembrane domains of AE2 both contribute to regulation of anion exchange by pH. J Biol Chem 271:5741–5749
57. Zhao R, Shin DS, Goldman ID (2011) Vulnerability of the cysteine-less proton-coupled folate transporter (PCFT-SLC46A1) to mutational stress associated with the substituted cysteine accessibility method. Biochim Biophys Acta 1808:1140–1145
58. Zhu Q, Azimov R, Kao L, Newman D, Liu W, Abuladze N, Pushkin A, Kurtz I (2009) NBCe1-A Transmembrane Segment 1 Lines the Ion Translocation Pathway. J Biol Chem 284:8918–8929
59. Zhu Q, Casey JR (2004) The substrate anion selectivity filter in the human erythrocyte Cl^-/HCO_3^- exchange protein, AE1. J Biol Chem 279:23565–23573
60. Zhu Q, Casey JR (2007) Topology of transmembrane proteins by scanning cysteine accessibility mutagenesis methodology. Methods (San Diego. Calif 41:439–450
61. Zhu Q, Kao L, Azimov R, Abuladze N, Newman D, Pushkin A, Liu W, Chang C, Kurtz I (2010) Structural and functional characterization of the C-terminal transmembrane region of NBCe1-A. J Biol Chem 285:37178–37187
62. Zhu Q, Kao L, Azimov R, Newman D, Liu W, Pushkin A, Abuladze N, Kurtz I (2010) Topological location and structural importance of the NBCe1-A residues mutated in proximal renal tubular acidosis. J Biol Chem 285:13416–13426
63. Zhu Q, Lee DW, Casey JR (2003) Novel topology in C-terminal region of the human plasma membrane anion exchanger, AE1. J Biol Chem 278:3112–3120
64. Zhu Q, Newman D, Kao L, Liu W, Azimov R, Kurtz I (2012) Insight into the structural differences in transmembrane segment 1 between NBCe1-A and AE1. FASEB J 689:683